

PPPL-2261

UC20-D,F,G

226
11/12/85 JS (2)

25

I-23815

PPPL-2261

PPPL--2261


DE86 002542

ON CONFINEMENT SCALING AND IGNITION IN TOKAMAKS

By

F.W. Perkins and Y.C. Sun

OCTOBER 1985

PLASMA
PHYSICS
LABORATORY 

DISTRIBUTION OF THIS DOCUMENT IS UNLIMITED

PRINCETON UNIVERSITY
PRINCETON, NEW JERSEY

PREPARED FOR THE U.S. DEPARTMENT OF ENERGY,
UNDER CONTRACT DE-AC02-76-CHO-3073.

ON CONFINEMENT SCALING AND IGNITION IN TOKAMAKS

F. W. Perkins and Y.C. Sun
Plasma Physics Laboratory, Princeton University
Princeton, New Jersey 08544

Abstract

A drift wave turbulence model is used to compute the scaling and magnitude of central electron temperature and confinement time of tokamak plasmas. The results are in accord with experiment. Application to ignition experiments shows that high density $(1-2) \cdot 10^{15} \text{cm}^{-3}$, high field, $B_T > 10 \text{ T}$, but low temperature $T \sim 6 \text{ keV}$ constitute the optimum path to ignition.

Anomalous electron thermal conductivity is the principal heat loss channel in most modern tokamaks. It has long been suspected that turbulent drift waves are the cause of anomalous thermal conductivity and a considerable literature has developed dealing with linear stability, nonlinear saturation, and experimental measurements of drift waves in tokamaks. Concurrently, tokamak experimentalists have been generating an extensive data base from which empirical scaling properties of confinement time and temperature with density, plasma current, toroidal field, minor and major radius, and so forth have been determined. Furthermore, the resulting empirical scalings are playing a crucial role in establishing the parameters of the next generation of tokamak experiments whose goal is to achieve ignition.

One is clearly motivated to ask: Are the empirical scalings in accord with the concept of drift wave turbulence? Are there hidden variables as yet unidentified in empirical scalings? Can the scaling properties of the present generation of experiments be safely extrapolated to the reactor regime? This work attempts a first answer to these questions, based on two general observations from tokamak experiments: First, drift wave amplitudes measured in tokamaks are in the strong turbulence regime, and, second, tokamak confinement is poor inside the $q = 1$ surface and outside the $q = 2$ surface. In other words, the region of effective thermal insulation lies between the $q = 1$ and $q = 2$ surfaces and, in this region, strong drift wave turbulence governs anomalous electron thermal conductivity.

Our approach to thermal transport by drift wave turbulence follows the spirit of earlier examples of transport in turbulent boundary layers which occur in fluid mechanics. One does not attempt to compute a turbulent transport coefficient from first principles, but instead, via rough physics arguments, one can construct transport coefficients which have physically correct scaling properties and an unknown, nondimensional, (but hopefully universal) multiplicative constant. The next step is to cast the heat transport equation into a nondimensional form, and, by solving it, obtain the numerical value of an eigenvalue which is a nondimensional combination of many physical quantities, including the unknown central electron temperature and universal constant. Comparison with experiment determines the constant. If the argument which deduces the transport coefficient is correct, then the universal constant must be found to be of order unity and the scaling properties of confinement time, etc. should agree with observation.

This approach brings out important qualitative trends bearing on the optimum avenue of approach to ignition. In a drift wave turbulence model, the anomalous thermal conductivity power losses rise rapidly with temperature, at least as rapidly as the increase of the D-T thermonuclear energy production above $T = 5$ keV. Consequently, temperatures in excess of $T = 6$ keV are not needed for ignition in tokamaks; additional heating results only in decreased confinement times. Drift wave turbulence models also indicate that confinement will be improved by high toroidal field, and, of course, thermonuclear energy production is enhanced by high density. Simple β -limit considerations show that shaped, high field tokamaks will permit very high central densities, given that the temperature does not have to exceed $T = 6$ keV. One concludes that ignition experiments should consider toroidal fields in the range 8-12 T and densities in the range $(1-4) \times 10^{15} \text{ cm}^{-3}$.

The confinement predictions of drift wave turbulence are quite sensitive to the shape of the density profile. This is the "hidden variable" of present-day confinement experiments. In the context of drift wave turbulence models, the difference between L-mode and H-mode tokamak thermal conductivities can be understood in terms of the flatness of the density profile. Unfortunately, a self-consistent determination of the density profile has not yet been developed, so the density profile shape is taken as a parameter in our model via the exponent α_n defined by

$$n = n_0 \left(1 - \frac{r^2}{a^2}\right)^{\alpha_n} \quad (1)$$

This sensitivity to profile shape rests on our strong turbulence model which posits that fine-scale turbulent $\vec{E} \times \vec{B}$ velocities must scale with the large-scale diamagnetic drift velocity

$$\frac{E_1 c}{B} = v_D = -c^{1/2} \frac{\tau_c}{eB} \frac{1}{n} \left(\frac{dn}{dr}\right) = c^{1/2} \frac{2Tc\alpha_n r}{eBa^2(1-r^2/a^2)} \quad (2)$$

Here, C denotes the universal constant to be determined from experiment.

It is expected that microinstability turbulence will not vanish completely as the density profile becomes flat, and that temperature-gradient modes will become the dominant microturbulent phenomena. Consequently, one should not assume that α_n can be very small in applying our results. Indeed, letting α_n decrease from $\alpha_n \approx 1$ to $\alpha_n \approx 0.3$ provides the correct decrease in thermal conductivity appropriate to the transition from L-mode to H-mode confinement.

Our confinement model¹ summarizes the observational Principle of Profile Consistency² for the relative electron temperature profile via the mathematical statements that the electron temperature is constant inside the $q = 1$ surface and falls to zero at the $q = 2$ surface. Because the current density follows the electron temperature profile, our temperature profiles fulfill the qualitative requirements for tearing mode stability.³ Hence confinement scaling depends on drift wave turbulence in the good confinement region between the $q = 1$ and $q = 2$ surfaces. In this region, magnetically trapped electrons execute random inward or outward $\vec{E} \times \vec{B}$ drifts. The random step size is governed by the trapped electron-drift wave coherence time τ_c , which, in turn, depends on the electron collision frequency. Two regimes naturally emerge: If the effective collision frequency ν_{eff} exceeds the diamagnetic drift frequency ω^* , then $\tau_c = \nu_{eff}^{-1}$, whereas, in the collisionless limit, $\tau_c = \omega^{*-1}$. Note that our definition of collisional, which can be written in terms of the conventional parameter ν^* as

$$\nu^* = \frac{\nu_{eff}}{\omega_{be}} > \left(\frac{m_e}{M_i}\right)^{1/2} \left(\frac{R}{a}\right)^{3/2} \frac{\alpha_n}{q_L^{1/4}} \approx 0.1, \quad (3)$$

differs from the usual definition of collisional: $v^* > 1$. [Additional numerical factors in our definition appear in Eq. (19) below.] The formulas for the electron thermal diffusivities χ_e are

$$\chi_{e1} = C_1 \frac{3T_e^{3.5} c_m^2 \alpha_n^{0.5} r^{3.5}}{(2\pi)^{0.5} e_B^2 n a^4 R^{1.5} (2Ln\Lambda) [1 - (r^2/a^2)]^2} \quad \text{collisional,} \quad (4)$$

$$\chi_{e2} = C_2 \frac{6T_e^{1.5} M_i^{0.5} c_r^{2.5} \alpha_n}{e_B^2 a^2 R^{0.5} (1 - r^2/a^2)} \quad \text{collisionless,} \quad (5)$$

In general, ohmic heating experiments lie in the collisional range whereas neutral beam injection (NBI) heating experiments are collisionless. Ignition experiments will be found to be collisional.

The next step is to introduce the electron heat balance equation

$$\frac{3}{2} \frac{1}{r} \frac{d}{dr} [r \chi_e n \frac{dT}{dr}] = \begin{array}{l} -j^2/\sigma \quad (\text{ohmic}) \\ -P/4\pi^2 R a r \quad (\text{NBI}) \end{array} \quad (6)$$

and cast it into a nondimensional form. The neutral beam power deposition profile models the PDX experiment.⁴ For collisional, ohmically heated plasmas, the resulting nondimensional equation is

$$\frac{1}{x} \frac{d}{dx} \left[\frac{x^{4.5}}{(1 - x^2/q_L)^2} \frac{dT}{dx} \right] = -\lambda_1 \tau^{1/3} \quad (7)$$

where

$$\tau = [T_e/T(0)]^{4.5} \quad x^2 = \alpha_L r^2/2a^2 \quad (8)$$

$$\lambda_1 = \frac{e_B^4 a^2 (2Ln\Lambda)^2}{16 C_1 \alpha_n^2 \gamma_E T(0)^6} \left(\frac{a}{R}\right)^{0.5} \left(\frac{q_L}{2}\right)^{0.75} \quad (9)$$

and γ_E denotes the Spitzer factor in the conductivity. Solutions of Eq. (7) determine the numerical value of λ_1 , which can be accurately fit by the formula $\lambda_1 = 5.1/q_L$. One then solves (9) for $T(0)$, obtaining a scaling law for central electron temperature. Numerical evaluation of the plasma energy content, coupled with the assumption $T_i = T_e$, leads to the scaling of the energy confinement time. In practical units, our results for ohmically heated plasmas are

$$T(0) = (0.80 \text{ keV}) \frac{(B_T^2 a_m Z)^{1/3}}{(C_1 \alpha_n^2)^{1/6}} \left(\frac{q_L}{3}\right)^{1/4} \left(\frac{3a}{R}\right)^{1/12} \quad (10)$$

$$\tau_E/\bar{n} = (0.16 \times 10^{-20} \text{ m}^3\text{-sec}) \frac{q_L R^{1.8} a_m}{(C_1 \alpha_n^2)^{0.42} B_T^{0.33} Z^{0.16}} \quad (11)$$

where B_T is the toroidal field in Tesla, and R_m , a_m are in meters. The prediction that $T(0)/Z^{1/3}$ should be independent of plasma density is borne out by experiments on TFTR.⁵ Indeed, Fig. 1 shows that the scaling trends of Eq. (10) match PLT and TFTR data well, although the best fit involves somewhat different exponents.⁵ Figure 2 shows that confinement time

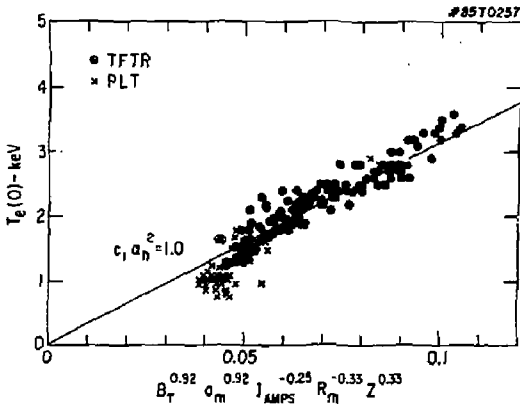


Fig. 1 Central electron temperature data from TFTR and PLT versus the theoretical formula of Eq. (10) with $C_1 \alpha_n^2 = 1.0$. Data supplied by G. Taylor.

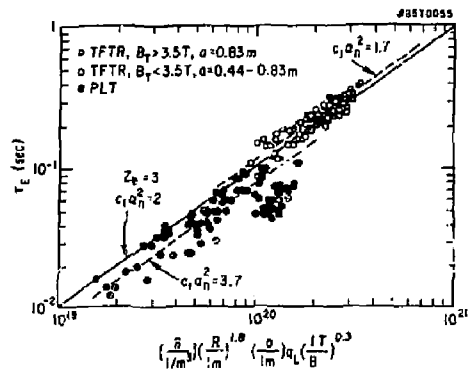


Fig. 2 Experimental energy confinement time τ_E for TFTR plotted against formula (11) for various values of $C_1 \alpha_n^2$ and for $Z_e = 3$. Data supplied by P. Efthimion and G. Taylor.

data from TFTR and PLT are well fit by $C_1 \alpha_n^2 \approx 2$. The fact that a higher value of $C_1 \alpha_n^2$ provides a better fit to PLT data ($C_1 \alpha_n^2 = 3.7$ for PLT versus $C_1 \alpha_n^2 = 1.7$ for TFTR) could arise from a consistently steeper density profile in PLT ($\alpha_n = 1.0$ versus $\alpha_n = 0.7$). This underscores the point that density profile flatness has been a hidden variable in confinement data. Figure 3 gives the temperature profiles computed in the numerical solutions of (7).

The difference in values of $C_1 \alpha_n^2$ needed to fit central electron temperature and confinement time data probably arises from the fact that the ion density is less than the electron density when Z_{eff} is significantly larger than unity.

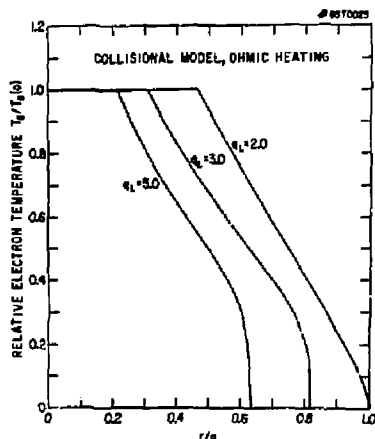


Fig. 3 Relative electron temperature profiles for ohmic heating computed from the solution of the nondimensional heat balance Eq. (7).

A similar procedure can be followed for NBI-heated tokamaks. In this case, the nondimensional equation is

$$\frac{1}{x} \frac{d}{dx} \left[\frac{x^{2.5}}{(1-x^2 \frac{2}{q_L})^{1-\alpha_n}} \frac{d\tau}{dx} \right] = - \frac{\lambda_2}{x}$$

where $\tau = (T_e/T(0))^{2.5}$ and λ_2 is

$$\lambda_2 = \left(\frac{5}{18 C_1 \alpha_n} \right) \frac{e^2 B^2 P}{4 \pi^2 T_e^{2.5} M_1^{0.5} C_2 n_0} \left(\frac{a}{R} \right)^{1/2} \left(\frac{q_L}{2} \right)^{1/4}$$

Numerical integrations yield $\lambda_2 = 0.70 (\alpha_n)^{-1/q_L}$. The resulting scaling for the central electron temperature and confinement time are

$$\tau(0) = 1.2 \text{ keV} \left[B_T \left(\frac{P}{n_{13}} \right)^{0.5} \right]^{0.8} \left(\frac{a}{AR C_2 \alpha_n} \right)^{0.2}, \quad (12)$$

$$\tau_E = \frac{3.3 \times 10^{-6} \text{ msec}}{(C_2 \alpha_n)^{0.4}} \left(\frac{\bar{n}_{13}}{P_{\text{MW}}} \right)^{0.6} \frac{a_{\text{cm}}^{0.4} R_{\text{cm}}^{1.7} I_{\text{kA}}^{0.9}}{B_T^{0.1}}. \quad (13)$$

Here \bar{n} is measured in units of 10^{13} cm^{-3} , R and a in cm, B_T in Tesla, I in kiloamps, P in megawatts, and A is the ion mass in AMU. Formula (13) has been compared with an extensive base of L-mode tokamak data.⁴ Figure 4 shows that a good fit results when $C_2 \alpha_n = 0.6$. A correspondingly good fit is obtained for the scaling of the central electron temperature, Eq. (12), as Fig. 5 shows.

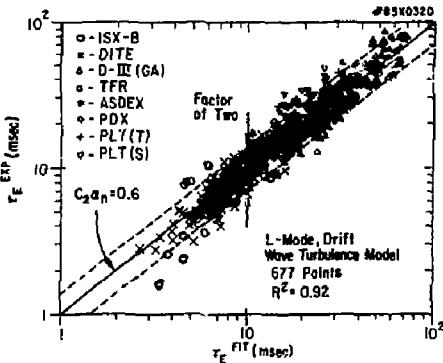


Fig. 4 Experimental energy confinement time for L-mode, NBI-heated tokamaks plotted against the theoretical fit (13). The solid line is expression (13) with $C_2 \alpha_n = 0.6$. This figure is adapted from Ref. 4.

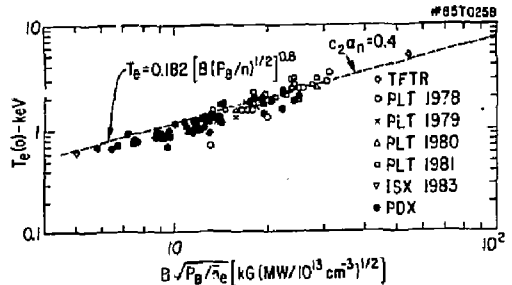


Fig. 5 Central electron data from L-mode NBI-heated tokamaks compared with Eq. (12). TFTR point was supplied by M. Murakami.

Figures 1 - 5 support the concept that strong drift wave turbulence is controlling electron thermal confinement in tokamaks. What does this imply for the ignition condition? We find that an ignition experiment will lie in the collisional regime, and that ignition will occur near $T = 6 \text{ keV}$. The ignition condition, based on a solution of the appropriate nondimensional heat

balance equation, which includes thermonuclear power production and bremsstrahlung losses, is

$$n_{15}^2 \left(\frac{B}{10T}\right)^2 a_m^{2.5} R_m^{1.5} > \left(\frac{7.3}{q_L}\right)^2 C_1 \alpha_n^2 \quad (14)$$

where n_{15} is the central electron density in units of 10^{15}cm^{-3} . Evidently, the ignition margin is sensitive to the flatness of the density profile. A value of $C_1 \alpha_n^2 = 0.5$ represents a reasonable optimum guess, in that flatter profiles and better confinement are observed in H-mode conditions. The inverse q_L dependence in (14) reflects the same physics as the positive q_L -dependence of confinement time in ohmically heated plasmas; both ohmic- and α -particle-heated tokamaks have heat sources that follow the relative temperature profile.

Ignition criterion (14) emphasizes high toroidal fields. Table I lists the parameters for two devices that achieve an ignition margin near unity.

Table I. Tokamak Parameters for an Ignition Margin Unity.

Parameter	I	II
B_T	12 T	8 T
k	1.3 m	3.5 m
$\bar{a} = (ba)^{1/2}$	0.65 m	1.0 m
q_L	3.6	3.6
$n(0)$	$1.7 \cdot 10^{15} \text{cm}^{-3}$	$0.7 \cdot 10^{15} \text{cm}^{-3}$
$\beta(0)$	0.04	0.05
$T(0)$	6 keV	6 keV
Ignition Margin	1.0	1.0
$C_1 \alpha_n^2$	0.5	0.5
Divertor	yes	yes
Bremsstrahlung	22 MW	23 MW

On a provisional basis, one should use the geometric mean minor radius in applying (14) to shaped tokamaks. We note that Device I is only 20% larger than the (BCX)² device proposed by B. Coppi.⁷ Let us further note that an

ignition tokamak must be a shaped tokamak to sustain a high central β -value, and to have sufficient plasma current to confine α -particles. Most likely, a divertor will be required to realize H-mode confinement implied by the choice $C_1 \alpha_n^2 = 0.5$.

Let us note that the central electron density proposed for Device I is roughly three times a Murakami limit based on bremsstrahlung radiation losses.⁸ Therefore, about 25 megawatts of auxiliary power is required to sustain this density while the temperature is being raised.

An ignition device may well have large, thermonuclear-driven sawtooth oscillations. The energy runaway time is only 0.60 sec for Device I, and confinement near the magnetic axis, apart from sawtooth oscillations, is excellent according to both experiment and the drift wave thermal diffusivity, Eq. (4). Because our confinement model assumed very high thermal conductivity inside $q = 1$, it fails to account for the energy content associated with the rise of a sawtooth and, therefore, yields a conservative estimate of the ignition margin.

Tokamak modeling computations require an explicit expression for the electron thermal diffusivity χ_e and a well-posed boundary condition for the thermal diffusivity calculations. The interpolation formula

$$\chi_e = \left(\frac{1}{\chi_1} + \frac{1}{\chi_2} \right)^{-1/2} \quad , \quad (15)$$

where

$$\chi_1 = C_1 \frac{3T_e^{3.5} c^2 m_e^{0.5}}{4(2\pi)^{0.5} e^6 B^2 n(z) \ln A} \left(\frac{r}{R} \right)^{1.5} \left(\frac{1}{n} \frac{dn}{dr} \right)^2 \quad , \quad (16)$$

$$\chi_2 = C_2 \frac{3 T_e^{1.5} M_i^{0.5} c^2}{e^2 B^2} \left(\frac{r}{R} \right)^{0.5} \left| \frac{1}{n} \frac{dn}{dr} \right| \quad , \quad (17)$$

should adequately describe the transition between the collisional and collisionless regimes. The recommended boundary condition is

$$T_e = 0.2 T_e(0) \text{ at } \begin{cases} q = 2 \text{ surface} & \text{L-Mode} \\ \text{separatrix} & \text{H-Mode} \end{cases} \quad . \quad (18)$$

In this case of L-mode tokamaks, the temperature profile is extended from the $q = 2$ surface to the limiter surface by a simple parabolic formula that ensures continuity of T_e and dT_e/dr of the $q = 2$ surface and sets $T_e = 0$ at the limiter surface. When Eq. (15) is used, the transition from collisionless to collisional physics takes place when the inequality

$$v^* = \frac{v_{el.}}{\omega_{ce}} = \frac{4(2\pi)^{1/2} q R^{2.5} n e^4 (z \ln \Lambda)}{3 r^{1.5} T_e^2} > \frac{q \left(\frac{R}{r}\right)^{3/2} \left(\frac{m_e}{m_i}\right)^{1/2} \frac{C_1}{C_2} r \left(\frac{dn}{dr}\right)} \quad (19)$$

is satisfied. Our normalization with experiment suggests the values $C_1 = 3$, $C_2 = 0.5$.

ACKNOWLEDGMENTS

This work has benefitted from discussions with P. Efthimion, H. Furth, R. Goldston, C.S. Liu, D. Meade, M. Murakami, P. Rutherford, W. Tang, G. Taylor, and R. Waltz. This work was supported by U.S. DOE Contract No. DE-AC02-76-CHO-3073.

REFERENCES

- ¹F. W. Perkins, "Confinement Scaling in Tokamaks: Consequences of Drift Wave Turbulence" in Proc. 4th Intl. Symp. on Heating in Toroidal Plasmas, Rome, 1984, Vol. 2, p. 977.
- ²B. Coppi, Comments Plasma Phys. Cont. Fusion 5, 261 (1980); R. J. Goldston, Plasma Phys. Cont. Fusion 26, 1A, 37 (1984).
- ³H. P. Furth, P. H. Rutherford, and H. Selberg, Phys. Fluids 16, 1054 (1973).
- ⁴S. M. Kaye et al., Nucl. Fusion 24, 1303 (1984). See Fig. 9.
- ⁵G. Taylor et al., "Evolution of the Electron Temperature Profile of Ohmically Heated Plasmas in TFTR," Princeton Plasma Physics Laboratory Report No. PPPL-2221, August 1985.
- ⁶S. M. Kaye, "A Review of Energy Confinement and Local Transport Scaling Results in Neutral Beam Heated Tokamaks" (unpublished).
- ⁷B. Coppi, "Advanced Fusion Burning Core Experiment" M.I.T. Research Laboratory of Electronics Report PTP-84/8, March 1984.
- ⁸F. W. Perkins and R. A. Hulse, Phys. Fluids 28, 1837 (1985).

REPRODUCED FROM
BEST AVAILABLE COPY

EXTERNAL DISTRIBUTION IN ADDITION TO UC-20

Plasma Res Lab, Austra Nat'l Univ, AUSTRALIA
Dr. Frank J. Paoloni, Univ of Wollongong, AUSTRALIA
Prof. I.R. Jones, Flinders Univ., AUSTRALIA
Prof. M.H. Brennan, Univ Sydney, AUSTRALIA
Prof. F. Cap, Inst Theo Phys, AUSTRIA
Prof. Frank Verheest, Inst theoretische, BELGIUM
Dr. D. Palumbo, Dg XII Fusion Prog, BELGIUM
Ecole Royale Militaire, Lab de Phys Plasmas, BELGIUM
Dr. P.H. Sakanaka, Univ Estadual, BRAZIL
Dr. C.R. James, Univ of Alberta, CANADA
Prof. J. Teichmann, Univ of Montreal, CANADA
Dr. H.M. Skarsgard, Univ of Saskatchewan, CANADA
Prof. S.R. Sreenivasan, University of Calgary, CANADA
Prof. Tudor W. Johnston, INRS-Energie, CANADA
Dr. Hannes Barnard, Univ British Columbia, CANADA
Dr. M.P. Bachynski, MFB Technologies, Inc., CANADA
Chalk River, Nucl Lab, CANADA
Zhengou Li, SW Inst Physics, CHINA
Library, Tsing Hua University, CHINA
Librarian, Institute of Physics, CHINA
Inst Plasma Phys, Academia Sinica, CHINA
Dr. Peter Lukac, Komenského Univ, CZECHOSLOVAKIA
The Librarian, Culham Laboratory, ENGLAND
Prof. Schatzman, Observatoire de Nice, FRANCE
J. Radet, CEN-EP6, FRANCE
AM Dupas Library, AM Dupas Library, FRANCE
Dr. Tom Mual, Academy Bibliographic, HONG KONG
Preprint Library, Cent Res Inst Phys, HUNGARY
Dr. S.K. Trehan, Punjab University, INDIA
Dr. Indra Mohan Lal Das, Banaras Hindu Univ, INDIA
Dr. L.K. Chavda, South Gujarat Univ, INDIA
Dr. R.K. Chhajlani, Vikram Univ, INDIA
Dr. B. Dasgupta, Saha Inst, INDIA
Dr. P. Kaw, Physical Research Lab, INDIA
Dr. Phillip Rosenau, Israel Inst Tech, ISRAEL
Prof. S. Cupezman, Tel Aviv University, ISRAEL
Prof. G. Rostagni, Univ Di Padova, ITALY
Librarian, Int'l Ctr Theo Phys, ITALY
Miss Clelia De Palo, Assoc EURATOM-ENEA, ITALY
Biblioteca, del CNR EURATOM, ITALY
Dr. H. Yamato, Toshiha Res & Dev, JAPAN
Dirac Dept. Gg. Tokamak Dev. JAERI, JAPAN
Prof. Nobuyuki Inoue, University of Tokyo, JAPAN
Research Info Center, Nagoya University, JAPAN
Prof. Kyoji Nishikawa, Univ of Hiroshima, JAPAN
Prof. Sigeno Mori, JAERI, JAPAN
Library, Kyoto University, JAPAN
Prof. Ichiro Kawakami, Nihon Univ, JAPAN
Prof. Satoshi Itoh, Kyushu University, JAPAN
Dr. D.I. Choi, Adv. Inst Sci & Tech, KOREA
Tech Info Division, KAERI, KOREA
Bibliotheek, Fom-Inst Voor Plasma, NETHERLANDS
Prof. B.S. Liley, University of Waikato, NEW ZEALAND
Prof. J.A.C. Cabral, Inst Superior Tecn, PORTUGAL
Dr. Octavian Petrus, ALI OJZA University, ROMANIA
Prof. M.A. Hallberg, University of Natal, SO AFRICA
Dr. Johar de Villiers, Plasma Physics, Nucor, SO AFRICA
Fusion Div. Library, JEN, SPAIN
Prof. Hans Wilhelmson, Chalmers Univ Tech, SWEDEN
Dr. Lennart Stanflo, University of UMEA, SWEDEN
Library, Royal Inst Tech, SWEDEN
Centre de Recherches, Ecole Polytech Fed, SWITZERLAND
Dr. V.T. Tolok, Kharkov Phys Tech Ins, USSR
Dr. D.D. Ryutov, Siberian Acad Sci, USSR
Dr. G.R. Eliseev, Kurchatov Institute, USSR
Dr. V.A. Glukhikh, Inst Electro-Physical, USSR
Institute Gen. Physics, USSR
Prof. T.J.M. Boyd, Univ College N Wales, WALES
Dr. K. Schindler, Ruhr Universität, W. GERMANY
Nuclear Res Estab, Julich Ltd, W. GERMANY
Librarian, Max-Planck Institut, W. GERMANY
Bibliothek, Inst Plasmaforschung, W. GERMANY
Prof. R.K. Janev, Inst Phys, YUGOSLAVIA

DISCLAIMER

This report was prepared as an account of work sponsored by an agency of the United States Government. Neither the United States Government nor any agency thereof, nor any of their employees, makes any warranty, express or implied, or assumes any legal liability or responsibility for the accuracy, completeness, or usefulness of any information, apparatus, product, or process disclosed, or represents that its use would not infringe privately owned rights. Reference herein to any specific commercial product, process, or service by trade name, trademark, manufacturer, or otherwise does not necessarily constitute or imply its endorsement, recommendation, or approval by the United States Government or any agency thereof. The views and opinions of authors expressed herein do not necessarily state or reflect those of the United States Government or any agency thereof.